INTERNATIONAL JOURNAL OF INTELLIGENT CONTROL AND SYSTEMS
VOL. 14, NO. 1, MARCH 2009, 33-40

Understanding the Role of Liver Zonation in Toxin Elimination

Shahab SHEIKH-BAHAEI, Sean H. J. KIM, Shahriar SHEIKHBAHAEI and C. Anthony HUNT

Abstract- **Using game theory and reinforcement learning, we created and analyzed generalized agent-based and compartmental models of hepatic toxin elimination processes to explore plausible causes of hepatic functional zonation. We considered a general situation in which a group of protective agents (analogous to liver cells) cooperate and self-organize their efforts to minimize optimally the negative effects of toxin intrusions. Following a totally different approach, we constructed a physiologically based model of a two-zoned liver to study the physiological consequences of zonation. The results of the two models support the hypothesis that liver zonation might be a consequence of an optimal strategy for toxin clearance.**

***Index Terms*—liver zonation, multi-agent learning, computational biology, self-organizing, *Q*-learning, game theory**

1. INTRODUCTION

The liver performs a wide range of functions including detoxification of blood-borne compounds. So doing protects the body. A human cannot live more than 24 hours without the liver. Hepatocytes, the parenchymal cells of the liver, are among the most complex cells in the body. They cooperate with each other to detoxify xenobiotics by metabolizing them to less toxic compounds. Over the course of their evolution they have learned to do so in an effective and optimal way. Hepatocytes express heterogeneous, location-dependent enzyme and transporter activities to facilitate detoxification, apparently following an intrinsic agenda, the principles of which are not fully understood. This phenomenon is known as liver zonation [1]. To gain insight into those processes, we constructed and analyzed a generalized problem of cooperative agents protecting their common wealth from harmful intruders. The agents are assumed to have incomplete information about each other and cannot form coalitions).

1.1 Biology Background

The liver is a complex biochemical factory which synthesizes, modifies, and metabolizes thousands of substances daily and provides the body with essential substances such as proteins and fats. The liver is also responsible for eliminating toxins and xenobiotics (including drugs) that find their way into blood. The rate of elimination, known as *hepatic clearance*, is different for each compound. Histologically, the liver is divided into lobules. Lobules consist of hepatocytes arranged in a roughly cylindrical or spherical shape. The central vein (CV), through which blood exits, is at the center. At the periphery are portal vein (PV) triads. A lobule is often described as being organized into three zones: periportal (upstream or zone 1), which encircles the portal tracts where blood enters, middle (zone 2), and perivenous (downstream or zone 3), which is poorly oxygenated and located around central vein. Oxygenated blood enters upstream, passes through the mid-zone, and exits downstream. Because of this spatial topology, different liver cells may not have the same exposure to incoming resources and compounds. For example, nutrients (e.g. oxygen) are more available to upstream than to the downstream cells.

Hepatocytes, although genetically identical, exhibit heterogeneous enzyme and transporter activities depending on their location within the lobule. For example, under normal conditions, hepatocytes located downstream express more enzymes for xenobiotic metabolism than do upstream hepatocytes. An obvious question is: why?

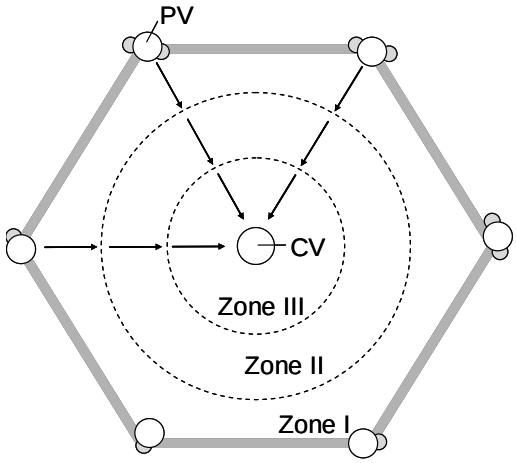

Fig 1. Cross section of a liver lobule. PV: portal triads, CV: central vein, arrows: direction of blood flow. Oxygenated blood enters the lobule from portal veins, and exits from central vein. Usually a liver lobule is described as being divided into three functional zones.

To represent hepatic metabolic zonation in physiologically based, pharmacokinetic models, researchers [2][3] usually divide the liver into compartments, each representing a different intrahepatic zone. Using a different approach, Lamers et al. [4] presents a "mechanistic

Manuscript received April 1, 2009. This work was supported in part by the CDH Research Foundation and a Graduate Fellowship to S. H. J. Kim from the International Foundation for Ethical Research. This paper is extended from "Multi-Agent Based Modeling of Liver Detoxification" published at *Spring Simulation Multiconference 2009, Agent-Directed Simulation Symposium,* San Diego, CA, USA, March, 2009.

Shahab Sheikh-Bahaei (e-mail: shahabsb@berkeley.edu) and S. H. J. Kim (e-mail: seanhjk@berkeley.edu) are with the UCSF/UC Berkeley Joint Graduate Group in Bioengineering, University of California, Berkeley, CA 94720, USA. Shahriar Sheikhbahaei (e-mail: shahriar@berkeley.edu) is with Department of Molecular and Cell Biology, University of California, Berkeley, CA 94720, USA

C. A. Hunt is with Department of Bioengineering and Therapeutic Sciences, University of California, San Francisco, CA 94143, USA (e-mail: a.hunt@ucsf.edu).

model" which proposes that zonation is induced by porto-central signal gradients.

2. METHODS

All existing models of liver zonation are top-down models. They fail to hypothesize elementary mechanisms that motivate the collective behaviors of liver cells.

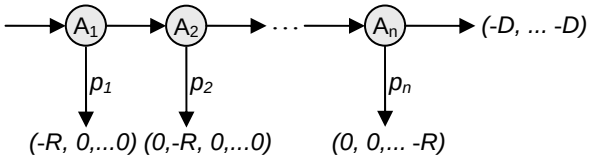

Fig 2. The game-theoretic model of the system. Agents either ignore or eliminate intruders. If Agent *i* (A_i) eliminates an intruder, it pays the cost of resource consumption (*R*). If all agents ignore an intruder, all must pay cost *D*, which is a consequence of damage caused by the intruder to the common wealth. p_i is the elimination strategy of agent i: it is the probability that A_i eliminates an incoming intruder. A_i's ability to eliminate is limited by $maxE_i\ (0 \le maxEi \le 1)$.

To understand the costs and benefits that may be associated with liver zonation, we began by using the game theoretic model as shown in Fig. 2: a sequence of *n* agents is protecting their common wealth (all extrahepatic tissues) against intruders. Agents are limited in their ability to eliminate intruders. The goal of each is to minimize potential damage caused by the intruders while minimizing resource consumption. What is the optimal elimination strategy for agent *i*? Obviously, an optimal strategy for agent *i* depends on the strategies of other agents who have the same goal.

Each agent has two options: eliminate or ignore an intruder. The immediate cost for elimination is resource consumption, denoted by R. Ignoring an intruder does not constitute an immediate cost; however, when all agents ignore an intruder (or it escapes for whatever reason), then all must pay the cost associated with any damage caused to the common wealth (denoted by *D*). It is assumed that a signal informs agents of the damage cost at the end of each round of play. Agent *i* cannot eliminate more than $maxE_i$ fraction of incoming intruders even if it expends maximum elimination effort $(0 \le maxEi \le 1)$. The elimination strategy of agent *i*, p_i, is the probability that it eliminates an incoming intruder. Agents who see intruders earlier, are called upstream agents; the others are called downstream agents.

To analyze the game's equilibrium, we first specified that there are only two agents. Their cost functions are calculated as follows:

$$e_1 = 1 - maxE_1 \cdot p_1$$

$$e_2 = (1 - maxE_2 \cdot p_2) \cdot e_1$$

where e_1 and e_2 are the fraction of intruders that escape from Agents 1 and 2. Expected average costs of damage to each agent will be:

$$ADC = e_2 \cdot D = (1 - maxE_2 \cdot p_2) \cdot e_1 \cdot D$$

Expected average costs of resource consumption are:

$$ARC_1 = maxE_1 \cdot p_1 \cdot R$$

$$ARC_2 = maxE_2 \cdot p_2 \cdot e_1 \cdot R$$

Total expected costs are:

$$<Cost_1> = ARC_1 + ADC = maxE_1 \cdot p_1 \cdot R + (1 - maxE_2 \cdot p_2)(1 - maxE_1 \cdot p_1) \cdot D$$

$$<Cost_2> = ARC_2 + ADC = maxE_2 \cdot p_2 \cdot (1 - maxE_1 \cdot p_1) \cdot R + (1 - maxE_2 \cdot p_2)(1 - maxE_1 \cdot p_1) \cdot D$$

$$<Cost_1> = maxE_1 \cdot p_1 \cdot (R - D) + \{1 - maxE_2 \cdot p_2 \cdot (1 - maxE_1 \cdot p_1)\} \cdot D \quad \text{(Eq.1)}$$

$$<Cost_2> = maxE_2 \cdot p_2 \cdot (1 - maxE_1 \cdot p_1)(R - D) + (1 - maxE_1 \cdot p_1) \cdot D \quad \text{(Eq.2)}$$

At any given location in the strategy space, agents have a preferred direction of movement to reduce their costs. For the two-player game, the direction can be described as a vector field based on the gradients of the above two cost functions:

$$u = -\frac{\partial <Cost_1>}{\partial p_1},\ v = -\frac{\partial <Cost_2>}{\partial p_2}$$

The vector field is shown in Fig. 3 for $n = 3$ and $D/R = 0.6$, 1.1, 1.7, 2.3, 3.7 and 10.0. It is easy to find the equilibrium of each game by inspecting its vector field. The figure shows that the equilibrium changes as D/R increases. When damage is very small ($D/R < 1$), all agents ignore because it is not cost effective to eliminate intruders. When damage is moderate, only downstream agents expend elimination effort. When damage is large, middle agents cooperate with the downstream agents. When damage is large enough, all agents expend elimination effort.

The analysis can be extended to a general case of *n* players as follows:

$$e_i = (1 - maxE_i \cdot p_i) \cdot e_{i-1} \quad i = 1, 2, \ldots, n \quad e_o = 1$$

$$ADC = e_n \cdot D$$

$$ARC_i = e_{i-1} \cdot maxE_i \cdot p_i \cdot R$$

$$<Cost_i> = ARC_i + ADC$$

$$<Cost_i> = e_{i-1} \cdot maxE_i \cdot p_i \cdot R + e_n \cdot D \quad \text{(Eq.3)}$$

where e_i is the fraction intruders that escape from agent *i*; *ADC* is the average damage cost to each agent; ARC_i is the average cost of resource consumption to agent *i*; and $<Cost_i>$ is the total expected cost (due to both actions) to agent *i*. The vector field can be calculated the same as for the two-player game, but it is infeasible to visualize and find equilibria. In general, analyzing equilibria of games involving three or more players is hard [5][6].

The above analysis requires that all agents have a priori knowledge about other agents and the environment. All the actions available to other agents and all costs with all combinations of actions are known by all agents. Consequently, it does not offer a mechanism through which autonomous agents can reach an optimal strategy.

We considered a more realistic situation in which agents do not have a priori information about their environment (including other agents). We used multi-agent simulation and enabled agents to learn from experience following a simple reinforcement learning rule. By keeping track of accumulated reward (and penalty), agents could be reinforced to learn an optimal clearance strategy. Their task was to maximize the long-term average reward per action.

The *Q*-learning algorithm [7], a well known reinforcement learning algorithm, has been shown to converge to an optimal decision policy. *Q*-learning has a solid foundation in the theory of Markov decision processes [8]. It is easy to implement and has been used widely in both single-agent and multi-agent contexts (see [8] and [9] for examples and [10] for a review of other multi-agent learning techniques).

Q-learning is a primitive form of learning [7] in which utility values (*Q* values) are learned for state-action pairs, absent a model of the environment. It provides a simple means for agents to learn how to act optimally in an unknown environment. At each step, a *Q*-learning agent uses its new experience to improve its long-term reward estimate by combining new information with prior experience.

Each *Q*-learning strategy is determined by the value function, *Q*, which estimates long-term discounted rewards for each action. General scheme of *Q*-learning algorithm used by each agent is as follows:

(1) Observe the current state (in this study, there is only one).
(2) Choose and execute an action based on the *Q*-values from a set of available actions, Act_i (available actions are Act_1 = eliminate and Act_2 = ignore). The agent selects its action according to a probability given by the Boltzmann distribution:

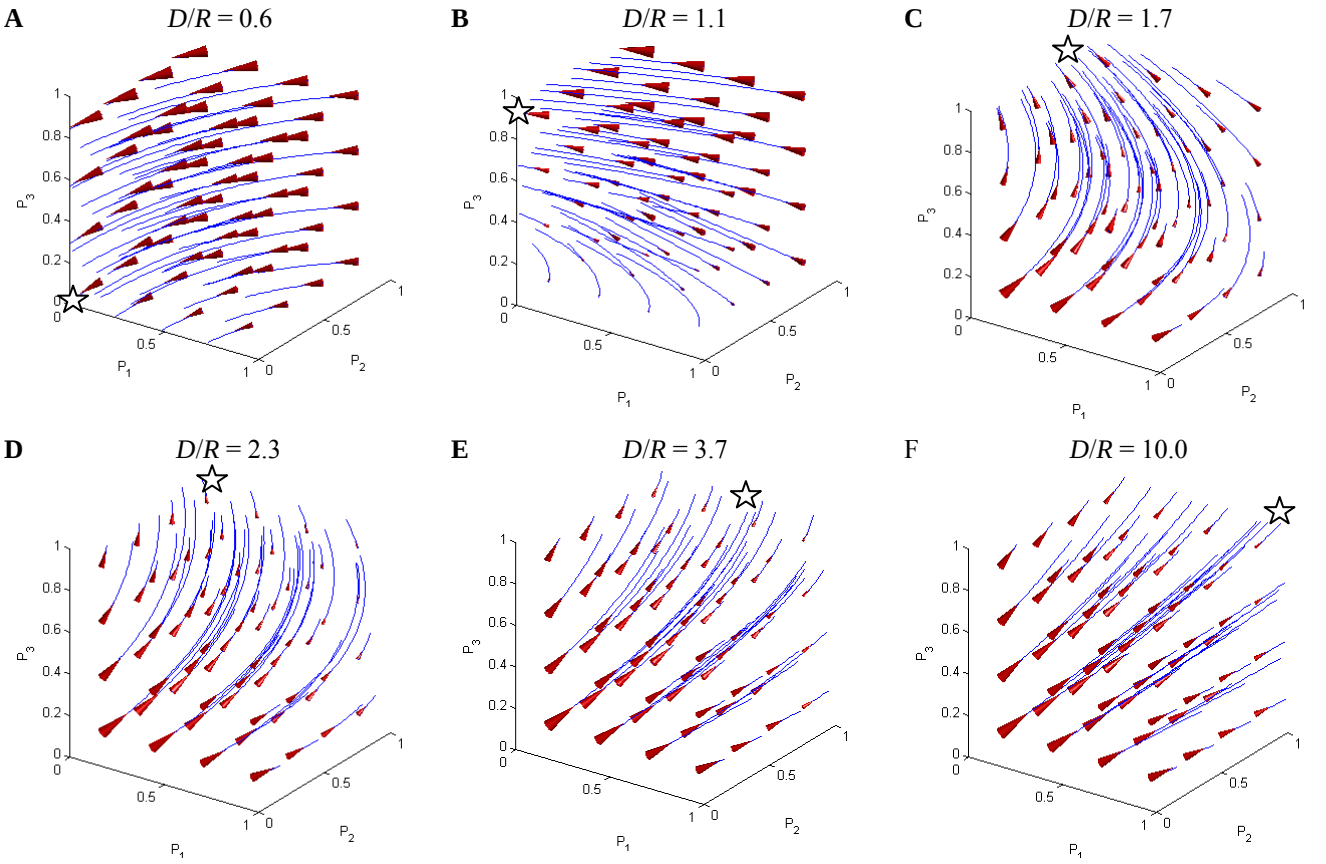

Fig 3. At any given non-equilibrium point in the strategy space, the agents have a preferred direction of moving in order to decrease their expected costs. The net direction towards which one moves in the strategy space depends on the slope of the cost functions at that point. Cone arrows show the net direction of movement when $n = 3$ and D/R ratio changes from 0.6 to 10.0. Each game's equilibrium is shown by a star. (A) D/R is small. In this case, all agents ignore the intruders. (B, C, D) D/R is moderately large; the equilibrium is such that Agent 1 ignores ($p_1 = 0$) but Agent 2 and 3 eliminate. (E, F) When D/R is large enough, Agent 1 starts making elimination effort.

$$p(Act_i) = \frac{e^{Q(Act_i)/T}}{\sum_{Act_k \in Actions} e^{Q(Act_k)/T}} \quad \text{(Eq. 4)}$$

where T, called "temperature," adjusts the randomness of decisions.

(3) Observe the new state (for this study, this step is not necessary because there is only one state) and receive an immediate reward.

(4) Adjust Q value based on the action taken, a, using Eq. 5:

$$Q(a) \leftarrow (1-\alpha)Q(a) + \alpha(reward + \beta V)$$
$$V = \max_b Q(b) \quad \text{(Eq.5)}$$

where α is the learning rate ($0 \le \alpha < 1$) and β is the discounting factor ($0 \le \beta < 1$). Here we specified $\alpha = 0.1$ and $\beta = 0.5$. V is known as the value of the game and is equal to the maximum Q value.

2.1. The Agent-Based Model

In mammalian livers, an absorbed toxin can be cleared by any of a sequence of hepatocytes. In order to gain insight into that process, we modeled the liver as consisting of many, parallel sets of toxin eliminating agents arranged in sequence from PV to CV in Fig. 1. Each agent used a Q-learning algorithm to decide its clearance strategy. An agents' task was to minimize the extrahepatic damage to the organism of which they are part. We specified that agents become aware of extrahepatic tissue damage via alarm signals that are quickly released into blood by the damaged tissue. Doing so was based on the fact that hepatocytes, like immune cells, express toll-like receptors [15]. They enable cells to detect chemical alarm signals generated by damaged tissues.

2.2 Physiologically-Based Model

In addition to the agent-based model, we used a traditional physiologically-based modeling approach to study the effects of hepatic zonation on toxicity exposure to the whole body (Fig. 4). For simplicity, the liver is represented as having two zones: periportal (zone 1) and perivenous (zone 2). Compounds in the liver are assumed to stochastically take one of the following four paths with probability p_i: Path 1: neither of the two zones encounters the compound. Path 2: only zone 1 encounters the compound. Path 3: both zones encounter the compound. Path 4: only zone 2 encounters the compound.

There is one set of differential equations for each path (Table A1). At each time step, one of the four sets is chosen according to the probability associated with the corresponding path. In this model, zone 1 and zone 2 eliminate compounds independent of each other. We specify that the mechanisms of xenobiotic elimination in the liver (including uptake transport, biliary efflux and metabolism) follow saturable Michaelis-Menten kinetics. Intrinsic clearance of each zone is specified to be $CL_i = V_{max,i}/Km$, where V_{max} is the maximum elimination (metabolic + transport) rate and Km is the Michaelis-Menten constant. V_{max} is assumed to be affected by the level of metabolic enzymes and transporters expressed by cells. As a result each zone has its own V_{max}. The two zones are specified to have equal Km values.

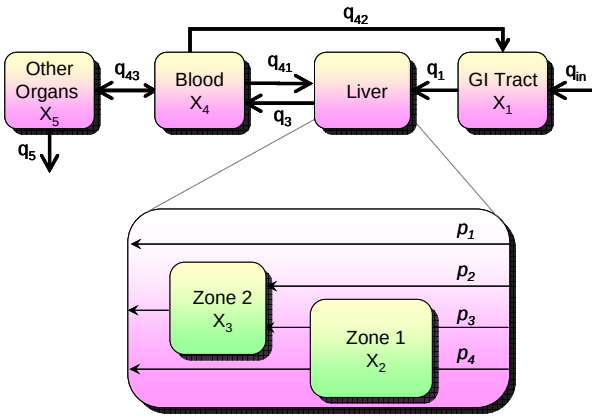

Figure 4. A physiologically-based model to analyze the effects of hepatic zonation on toxicity exposure to the whole body. Boxes are reservoir compartments. Arrows show xenobiotic flow directions. q's are xenobiotic flow rate constants. X_i's are xenobiotic concentration in corresponding reservoir compartment shown. p_i is the probability that xenobiotic passes through path i.

Further, we represent the cost to the organism, J, as being proportional to $(CL_1)^2 + (CL_2)^2 + (cAUBC)^2$, where CL_1 and CL_2 are intrinsic periportal clearance and intrinsic perivenous clearance, respectively; AUBC is the area under the blood concentration curve and c adjusts the relative cost contribution of a fixed dose based on xenobiotic toxicity.

3. RESULTS

Figure 5 shows the emergent strategies obtained for different values of D/R. When D/R is small, agents expend little effort to eliminate intruders. As D/R increases, downstream agents expend more elimination effort than upstream agents. When D/R is large, upstream agents begin cooperating and contribute to the elimination process, until all agents are expending maximum effort. Although the downstream agents always expend an equal or greater effort than do upstream agents, it does not mean that downstream agents actually eliminate more intruders. For example, when $D/R = 5.0$, upstream agents eliminate more intruders than do downstream agents.

Figure 6 shows the results from the physiologically based model. Figure 6A shows a typical 3D surface of the cost function, J, when c = 0.1. At that toxicity value, the minimum cost (J_{min}) occurs when $CL_1 = 0.35$ and $CL_2 = 0.45$ (i.e. zone 2 expends more clearance effort than zone 1). What happens if toxicity is altered? Figure 6B shows how J_{min} changes if toxicity varies from 0.05 to 5. It depicts as toxicity increases, both CL_1 and CL_2 increase however CL_2 is greater or equal to CL_1 at all toxicity levels. That observation is consistent with the game theoretic and multi-agent models results.

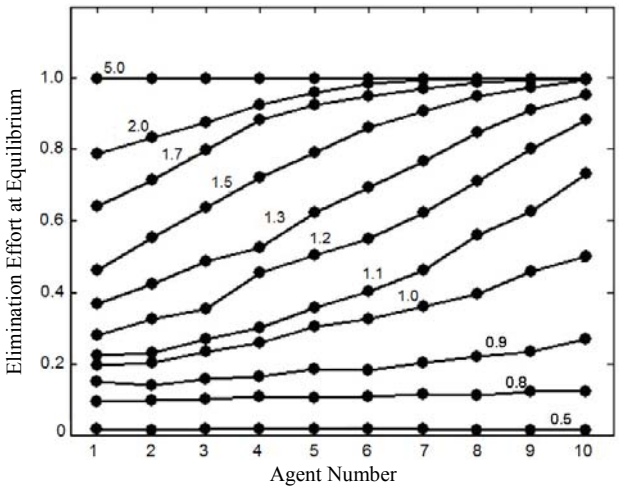

Fig 5. Equilibrium of the *n*-player game changes with *D*. Upstream is to the left (small numbers) and downstream is to the right. The average elimination strategies of 10 agents are shown for different ratios of *D*/*R* (shown on each curve) after 10,000 simulation steps ($maxE_i$ = 0.05). When *D*/*R* is small, upstream and downstream agents expend little elimination effort. As *D*/*R* ratio increases, downstream agents expend more elimination effort than upstream agents. When *D*/*R* is large, upstream agents start to cooperate and contribute to the elimination process.

4. VALIDATION

Liver cells exhibit a similar behavior: they express heterogeneous, location-dependent enzyme and transporter activities to detoxify compounds. Downstream cells commit most to toxin elimination; in other words, xenobiotic metabolism is preferentially located downstream, in the perivenous region [1]. The model also suggests that the location of hepatotoxicity depends on compound toxicity: less toxic compounds are likely to damage the downstream region, whereas compounds that are more toxic are more likely to damage the upstream region. Several highly toxic compounds [11], such as TCDD (LD50 = 0.034 mg/kg), cyclochlorotine (LD50 = 2-3 mg/kg), and gossypol (LD50 = 5 mg/kg), selectively damage the upstream zone [12-14]. On the other hand, less toxic compounds such as acetaminophen (LD50 = 1295 mg/kg) selectively damage the downstream zone [11].

5. DISCUSSION

We presented a simple, agent-based model of a generalized, hepatic xenobiotic clearance process. The model consists of a group of agents that, similar to hepatocytes, cooperate to protect a common wealth against toxic intruders. The agents do not have a priori information about either the environment or other agents (e.g., the number of other agents, actions available to them, costs associated with their actions, etc.). The agents use *Q*-learning, a primitive form of learning, to minimize their long-term discounted costs. Agents are assumed to know the cost of their own actions. We also assume that relatively fast communication mechanisms provide appropriate danger signals to agents, informing them about damage caused. Furthermore, agents are assumed to take and use the best policy.

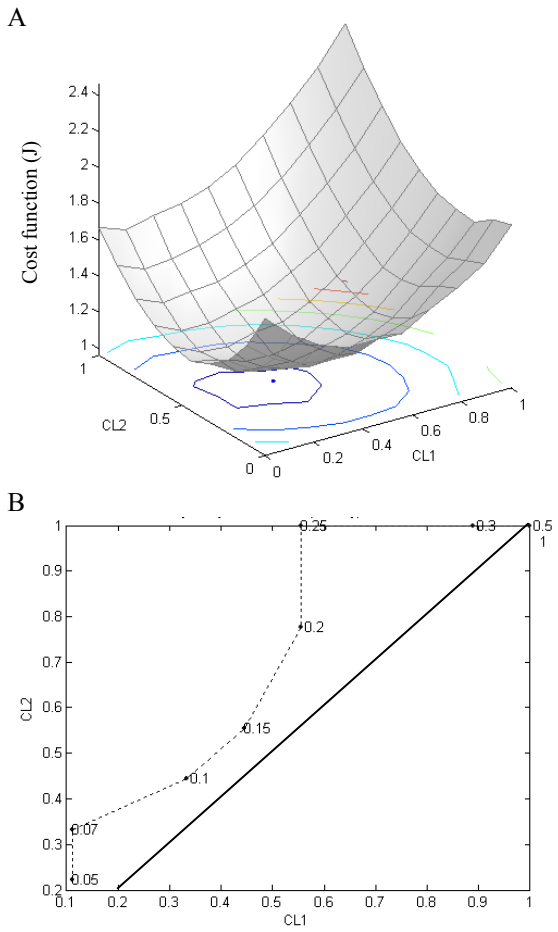

Fig 6. Effects of toxicity change in the physiologically-based model. (A) 3D plot of cost function, J, versus CL_1 and CL_2, when c = 0.1. (B) Dotted curve: trajectory of J_{min} as c changes from 0.05 to 0.5. For each point on the trajectory the value of corresponding c is reported. Solid line: the unity line.

Simulations showed that agents adjust their clearance effort based on the following two factors: the potential damage caused by intruders, and their ranked proximity to the entity being protected. Downstream agents (the ones with less proximity to the common wealth) generally expend more elimination effort than do upstream agents, depending on the threat.

The emergent, collective behaviors of these agents are similar to those of hepatic cells in terms of xenobiotic clearance. The model suggests that an underlying mechanism responsible for liver zonation may be similar to the model's simple mechanism. Hepatocytes may possess subsystems (e.g. special proteins, signaling pathways, etc.) that produce phenomena that have properties that are indistinguishable from those of the *Q*-learning algorithm.

Can hepatocytes learn? At the molecular level, short-term memory (persistent for weeks) within brain forms in

part by changing the strength of existing synaptic contacts. It can be achieved by altering the amount of neurotransmitter released from presynaptic terminals and/or postsynaptic receptor concentrations [17]. Simply stated, the molecular mechanism of learning involves adaptation of synaptic strength based on feedback signals received from other neurons [18]. Hepatocytes exhibit complex behavior. Recent studies show that toxin-induced hepatocyte injury is not a simple passive process regulated by the dose of an inducer compound; rather it is an active process in which active signaling plays a crucial role [19]. Hepatocytes change protein expression levels in response to toxic shocks [1] and adjust their sensitivity to signaling molecules (for example see [20] and [21]). Upstream hepatocytes can communicate with downstream hepatocytes via blood borne signals [4] and/or intercellular calcium waves [22-23]. On the other hand, downstream cells can communicate back with upstream cells via bile acids [24]. This bi-directional communication creates a complex intercellular feedback system which might contribute to regulation of adaptation (learning) in the liver.

ACKNOWLEDGEMENT

We thank Prof. Yoav Shoham and members of the UCSF BioSystems Group for helpful suggestions and discussions. We gratefully acknowledge research funding provided by the CDH Research Foundation and a Graduate Fellowship (SHJK) from the International Foundation for Ethical Research.

REFERENCES

[1] K. Jungermann, "Zonation of metabolism and gene expression in liver." Histochem. Cell Biol., vol. 103, pp. 81-91, 1995.
[2] T. N. Abu-Zahra and K. S. Pang, "Effect of Zonal Transport and Metabolism on Hepatic Removal: Enalapril Hydrolysis in Zonal, Isolated Rat Hepatocytes In Vitro and Correlation with Perfusion Data," Drug. Metab. Dispos., vol. 28, pp. 807-813, 2000.
[3] M. R. Gray and Y. K. Tam, "The series-compartment model for hepatic elimination," Drug Metab. Dispos., vol. 15, pp. 27-31, 1987.
[4] W. H. Lamers, T. Grange, A. F. Moorman, J. M. Ruijter, H. Sassi and V. M. Christoffels, "A mechanistic model for the development and maintenance of portocentral gradients in gene expression in the liver." Hepatology, vol. 29, pp. 1180-92, 1999.
[5] C. Daskalakis and C. H. Papadimitriou. (2005, Three-player games are hard. Electron. Colloq. Comput. Complexity 139
[6] C. Daskalakis, P. W. Goldberg and C. H. Papadimitriou, "The complexity of computing a nash equilibrium," in 2006, pp. 71-78.
[7] Watkins, Christopher J. C. H. and P. Dayan, "Technical Note: Q-Learning," Mach. Learn., vol. 8, pp. 279-292, 1992.
[8] J. Hu and M. P. Wellman, "Nash q-learning for general-sum stochastic games," Journal of Machine Learning Research, vol. 4, pp. 1039-1069, 2003.
[9] E. Yang and D. Gu, "Multiagent Reinforcement Learning for Multi-Robot Systems: A Survey." 2004.
[10] Y. Shoham, R. Powers and T. Grenager, "If multi-agent learning is the answer, what is the question?" Artificial Intelligence, vol. 171, pp. 365-377, 2007.
[11] TOXNET US Nat'l Library of Medicine, 2008. http://toxnet.nlm.nih.gov/. Accessed 05/2008
[12] L. S. Birnbaum, S. K. Alcasey, G. W. Lucier, K. O. Lindros, J. Blanton, N. J. Walker, V. M. Richardson and M. J. Santostefano, "Dose-dependent localization of TCDD in isolated centrilobular and periportal hepatocytes." Toxicol. Sci., vol. 52, pp. 9-19, 1999.
[13] T. Tatsuno, E. Ito and K. Terao, "Liver injuries induced by cyclochlorotine isolated from Penicillium islandicum." Arch. Toxicol., vol. 55, pp. 39-46, 1984.
[14] Y. C. Lin, D. C. Nuber and S. Manabe, "Zone-specific hepatotoxicity of gossypol in perfused rat liver." Toxicon, vol. 29, pp. 787-90, 1991.
[15] T. R. Billiar, Y. Vodovotz, D. A. Geller, A. N. Salyapongse and S. Liu, "Hepatocyte toll-like receptor 2 expression in vivo and in vitro: role of cytokines in induction of rat TLR2 gene expression by lipopolysaccharide." Shock, vol. 14, pp. 361-5, 2000.
[16] M. Hosseini-Yeganeh and A. J. McLachlan, "Physiologically Based Pharmacokinetic Model for Terbinafine in Rats and Humans," Antimicrob. Agents Chemother., vol. 46, pp. 2219, 2002.
[17] E. R. Kandel and J. H. Schwartz, "Molecular biology of learning: modulation of transmitter release," Science, vol. 218, pp. 433-443, 1982.
[18] E. R. Kandel, J. H. Schwartz and T. M. Jessell, Essentials of Neural Science and Behavior. Appleton & Lange, 1995,
[19] B. E. Jones and M. J. Czaja, "Intracellular signaling in response to toxic liver injury," Am. J. Physiol. Gastrointest. Liver Physiol., vol. 275, pp. 874-878, 1998.
[20] Y. Xu, B. E. Jones, D. S. Neufeld and M. J. Czaja, "Glutathione modulates rat and mouse hepatocyte sensitivity to tumor necrosis factor α toxicity," Gastroenterology, vol. 115, pp. 1229-1237, 1998.
[21] S. Herrmann, M. Seidelin, H. C. Bisgaard and O. Vang, "Indolo [3, 2-b] carbazole inhibits gap junctional intercellular communication in rat primary hepatocytes and acts as a potential tumor promoter," Carcinogenesis, vol. 23, pp. 1861, 2002.
[22] G. DUPONT, T. TORDJMANN, C. CLAIR, S. SWILLENS, M. CLARET and L. COMBETTES, "Mechanism of receptor-oriented intercellular calcium wave propagation in hepatocytes," FASEB J., vol. 14, pp. 279-289, 2000.
[23] V. Serrière, B. Berthon, S. BOUCHERIE, E. Jacquemin, G. Guillon, M. Claret and T. Tordjmann, "Vasopressin receptor distribution in the liver controls calcium wave propagation and bile flow 1," FASEB J., vol. 15, pp. 1484-1486, 2001.
[24] R. Gebhardt and F. Gaunitz, "Cell-cell interactions in the regulation of the expression of hepatic enzymes," Cell Biol. Toxicol., vol. 13, pp. 263-273, 1997.

Shahab Sheikh-Bahaei received B.S. degree in Electrical Engineering in Dec. 1999 from Isfahan University of Technology, Isfahan, Iran; and M.S. degree in Control Engineering in Dec. 2003 from University of New Mexico, Albuquerque, USA. He is currently a doctoral candidate in the UCSF/UC-Berkeley Joint Graduate Group in Bioengineering at University of California, San Francisco and Berkeley. His areas of interest include modeling and simulation, multi-agent systems, self-organizing systems, complex systems modeling and artificial intelligence.

Sean H. J. Kim received B.A. degree in computer science and mathematics in 2001 from University of California, Berkeley, USA. He is currently a doctoral student in the UCSF/UC Berkeley Joint Graduate Group in Bioengineering at University of California, San Francisco and Berkeley. His research interests include multi-agent, discrete event-oriented modeling and simulation, systems biology, theoretical formalisms for biology, and computational methods in drug development. His technical knowledge draws from previous software engineering experience at Cadence Design Systems and Avanti Corporation in the electronic design automation industry.

Shahriar Sheikhbahaei will receive B.A. degree in molecular and cell biology with a concentration on neurobiology in 2009 from University of California, Berkeley, USA. His current research is on plasticity of neuronal synapses. His research interests include synaptic plasticity, cellular and molecular neurobiology, developmental neurobiology, neurogenetics and mechanisms of nervous system structure and function.

C. Anthony Hunt received B.S. degrees in Chemistry and Applied Biology from the Georgia Institute of Technology and the Ph.D. degree from the University of Florida. His research transitioned from wet-lab to computational in 1998. He directs the BioSystems Group. The group's research focuses on developing and using advanced modeling and simulation methods to help unravel the complexities of biological systems used in biomedical and pharmaceutical research. Dr. Hunt is a member of several scientific and engineering societies, including ACM, IEEE Engineering in Medicine and Biology Society, Society for Computer Simulation International, and Biomedical Engineering Society. He is a member and fellow of the American Association for the Advancement of Science and the American Association of Pharmaceutical Scientists.

Appendix

Table A1. Equations of the model for each of the four paths shown in Figure 4.

Path 1	$V_1 \frac{dx_1}{dt} = -q_1 x_1 + q_{42} x_4 + q_{in}$ $V_4 \frac{dx_4}{dt} = q_1 x_1 - (q_{42} + q_{43}) x_4$ $V_5 \frac{dx_5}{dt} = q_{43} x_4 - q_5 x_5$
Path 2	$V_1 \frac{dx_1}{dt} = -q_1 x_1 + q_{42} x_4 + q_{in}$ $V_2 \frac{dx_2}{dt} = q_1 x_1 - q_3 x_2 - \frac{V\max_1 x_2}{Km_1 + x_2} + q_{41} x_4$ $V_4 \frac{dx_4}{dt} = q_3 x_2 - (q_{41} + q_{42} + q_{43}) x_4$ $V_5 \frac{dx_5}{dt} = q_{43} x_4 - q_5 x_5$
Path 3	$V_1 \frac{dx_1}{dt} = -q_1 x_1 + q_{42} x_4 + q_{in}$ $V_2 \frac{dx_2}{dt} = q_1 x_1 - q_2 x_2 - \frac{V\max_1 x_2}{Km_1 + x_2} + q_{41} x_4$ $V_3 \frac{dx_3}{dt} = q_3 x_2 - q_3 x_3 - \frac{V\max_2 x_3}{Km_2 + x_3}$ $V_4 \frac{dx_4}{dt} = q_3 x_3 - (q_{41} + q_{42} + q_{43}) x_4$ $V_5 \frac{dx_5}{dt} = q_{43} x_4 - q_5 x_5$
Path 4	$V_1 \frac{dx_1}{dt} = -q_1 x_1 + q_{42} x_4 + q_{in}$ $V_3 \frac{dx_3}{dt} = q_1 x_1 - q_3 x_3 - \frac{V\max_2 x_3}{Km_2 + x_3} + q_{41} x_4$ $V_4 \frac{dx_4}{dt} = q_3 x_3 - (q_{41} + q_{42} + q_{43}) x_4$ $V_5 \frac{dx_5}{dt} = q_{43} x_4 - q_5 x_5$

Model Parameters. Volumes of distribution: The apparent volume of distribution differs from compound to compound and from organ to organ. We assume that the model compartments are well-stirred and substrates instantly distribute in the entire tissue volume. The volumes of organs are reported for a 250-g rat in Table A.2.

V_1 = Volume of G.I Tract (V_{gi}) = $V_{stomach}$ + $V_{small\ intestine}$ + V_{spleen}

V_2 = Volume of zone 1 (V_{z1}) = (3/4) V_{Liver} *

V_3 = Volume of zone 2 (V_{z2}) = (1/4) V_{Liver} *

V_4 = Volume of blood (Vb)= $V_{arterial\ blood}$ + $V_{venous\ blood}$

V_5 = Volume of other organs = $V(muscle + skin + adipose + heart + kidney)$

Table A.2. Physiological parameters of tissues in a 250-g rat [16].

Tissue	V (ml)	Q (ml/min)
G.I.Tract	13.1	9.8
Liver	10.3	11.8
Blood	16.9	43
Other	176.9	n/a

Rate constants:

q_1= blood flow of G.I. Tract (Qgi)

q_3=hepatic blood flow (QL)

q_{41}=hepatic arterial flow (QL-Qgi)

q_{42}=G.I. Tract blood flow (Qgi)

q_{43}=effective flow of substrates from blood to other organs which we assume is generally less than the sum total blood flow of the organs.

$q5$=clearance rate of xenobiotics from blood by other organs which is primarily done by kidney (renal clearance).

The rate constants are listed in Table A3.

* If the liver lobule is roughly approximated as a cylinder (radius r and height h) with two zones, then zone 2 (perivenous) could be thought of as a smaller cylinder with radius r/2. The rest of the volume would represent zone 1 (perportal). The ratio of the two volumes can be calculated as follows:
Volume of zone 1 = $V_{z1} = 2h\pi r^2 - h\pi r^2$; Volume of zone 2 = $V_{z2} = h\pi r^2$; $V_{z1}/V_{total} = 3\pi r^2/4\pi r^2 = 3/4$; and $V_{z2}/V_{total} = \pi r^2/4\pi r^2 = 1/4$

Table A3. Rate constant values.

Parameter	Value
q_1	9.8 (=Qgi)
q_3	11.8 (=QL)
q_{41}	2.0 (=QL-Qgi)
q_{42}	9.8 (=Qgi)
q_{43}	1
q_5	0.5

Metabolic Enzymes (*V*max and *Km*): We assume that the mechanisms of xenobiotic elimination in the liver (including uptake transport, biliary efflux and metabolism) are saturable. We represent the mechanisms using Michaelis-Menten kinetics.